Supplement of Geosci. Model Dev., 16, 5153–5178, 2023
https://doi.org/10.5194/gmd-16-5153-2023-supplement


Geoscientific Model Development
Open Access
EGU

*Supplement of*

# Simulated stable water isotopes during the mid-Holocene and pre-industrial periods using AWI-ESM-2.1-wiso

**Xiaoxu Shi et al.**

*Correspondence to:* Martin Werner (martin.werner@awi.de)

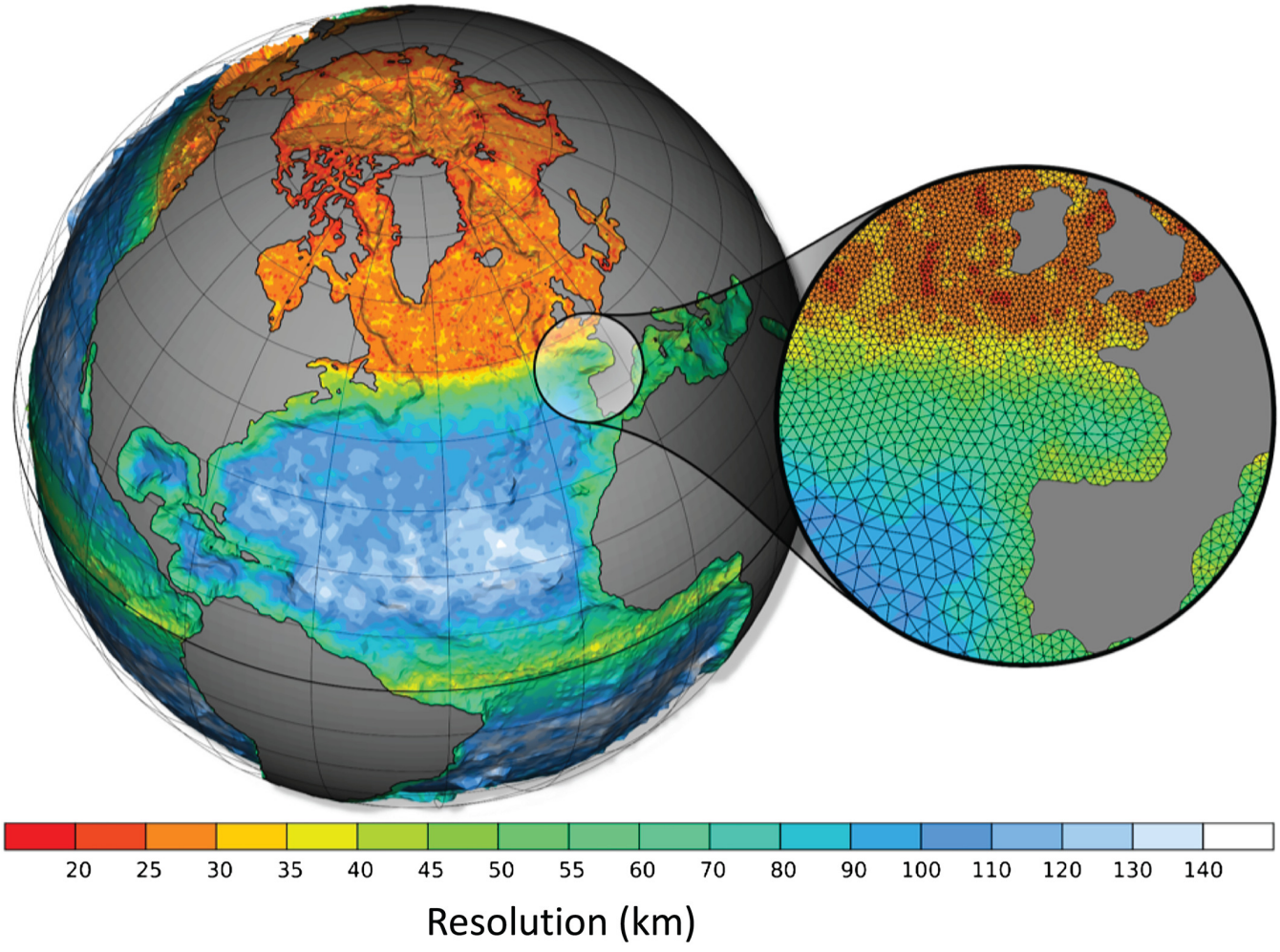


**Figure S1.** Resolution of ocean grid.

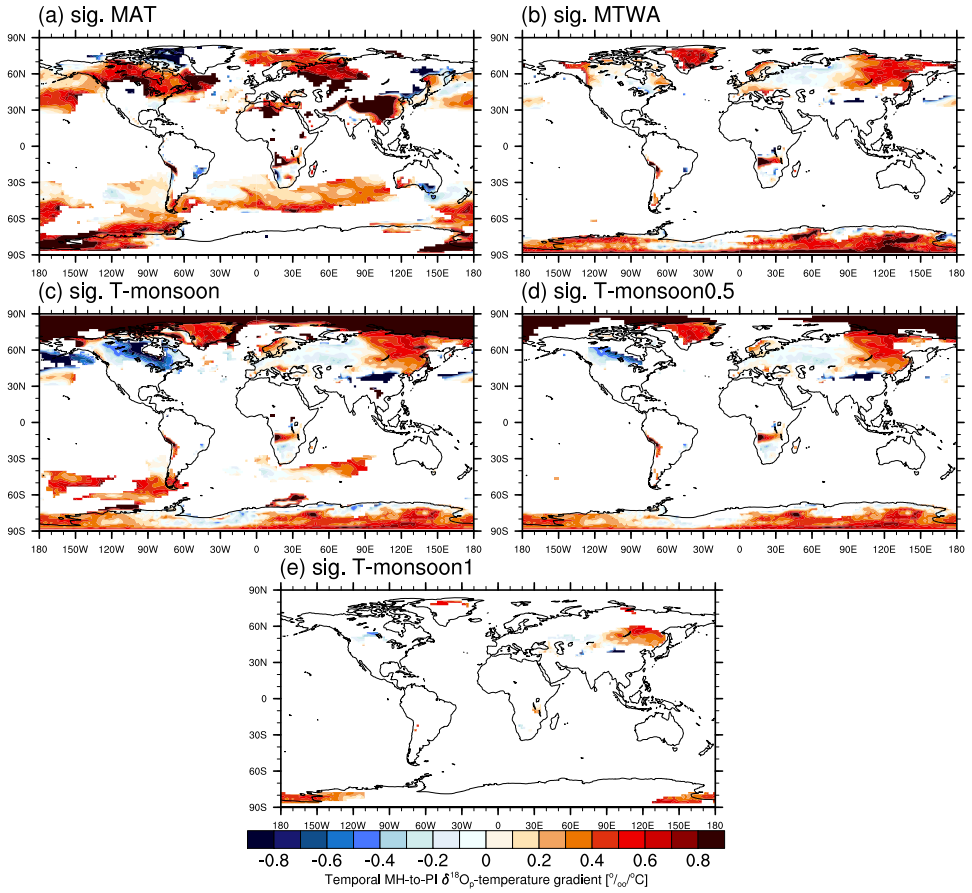


**Figure S2.** (a) Simulated temporal MH-to-PI $\delta^{18}O_p$-temperature gradient for all grid boxes with mean annual temperature (MAT) for both PI and MH being lower than 20 $^{\circ}C$ and the change in temperature between MH and PI is significant based on Student's t-test. (b) Same as in (a), but using the temperature of the warmest month (MTWA). (c) Same as in (a) but using the temperature of the monsoon months (JJAS for the Northern Hemisphere, DJFM for the Southern Hemisphere). (d) Same as in (c) but only for the areas with a temperature anomaly being larger than 0.5 °C. (e) Same as in (c) but only for the areas with a temperature anomaly being larger than 1 °C Units: $‰/^{\circ}C$.

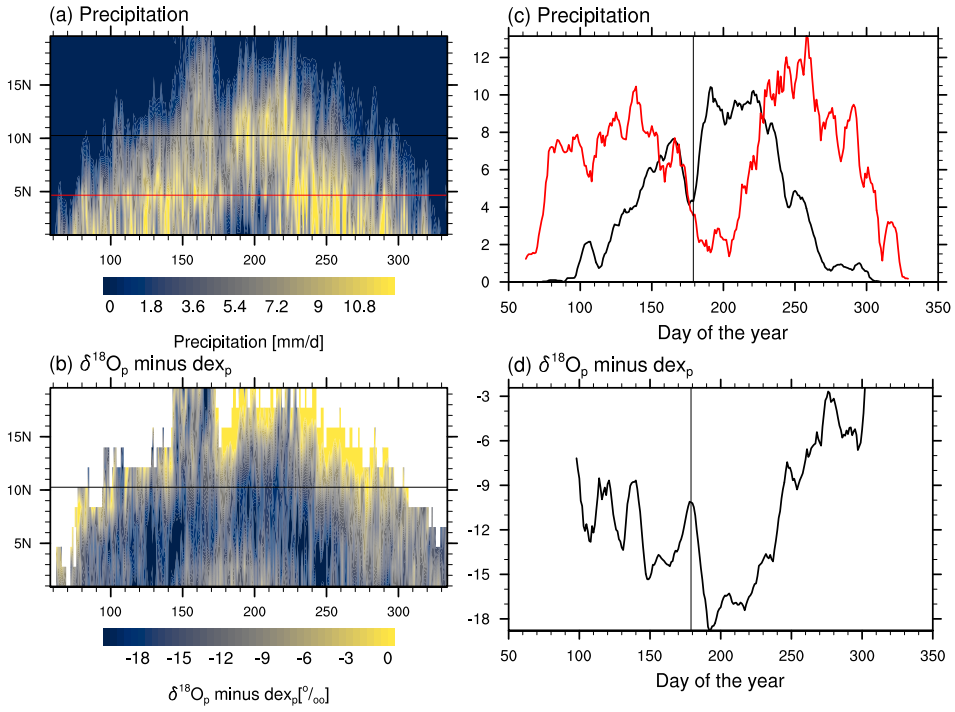


**Figure S3.** Simulated temporal time–latitude diagram of daily (a) precipitation and (b) $I$ averaged over 15°W - 20°E under MH climate condition for a specific year, with x-axis representing the day of the year and y-axis the latitude. (c) Time sections of precipitation averaged over 15°W - 20°E at 10.3°N (black line) and at 4.7°N (red line), filtered with high frequency variability (period less than 10 days) removed. (d) Time sections of $I$ averaged over 15°W - 20°E at 10.3°N, filtered with high frequency variability (period less than 10 days) removed.

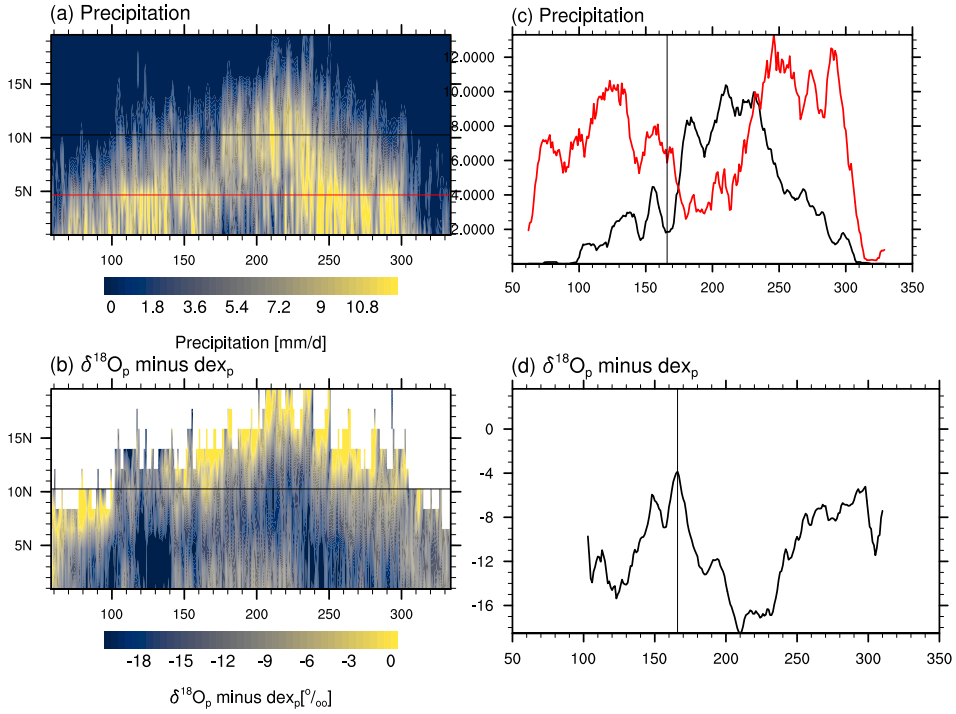


**Figure S4.** Simulated temporal time–latitude diagram of daily (a) precipitation and (b) $I$ averaged over 15°W - 20°E under MH climate condition for a specific year, with x-axis representing the day of the year and y-axis the latitude. (c) Time sections of precipitation averaged over 15°W - 20°E at 10.3°N (black line) and at 4.7°N (red line), filtered with high frequency variability (period less than 10 days) removed. (d) Time sections of $I$ averaged over 15°W - 20°E at 10.3°N, filtered with high frequency variability (period less than 10 days) removed.

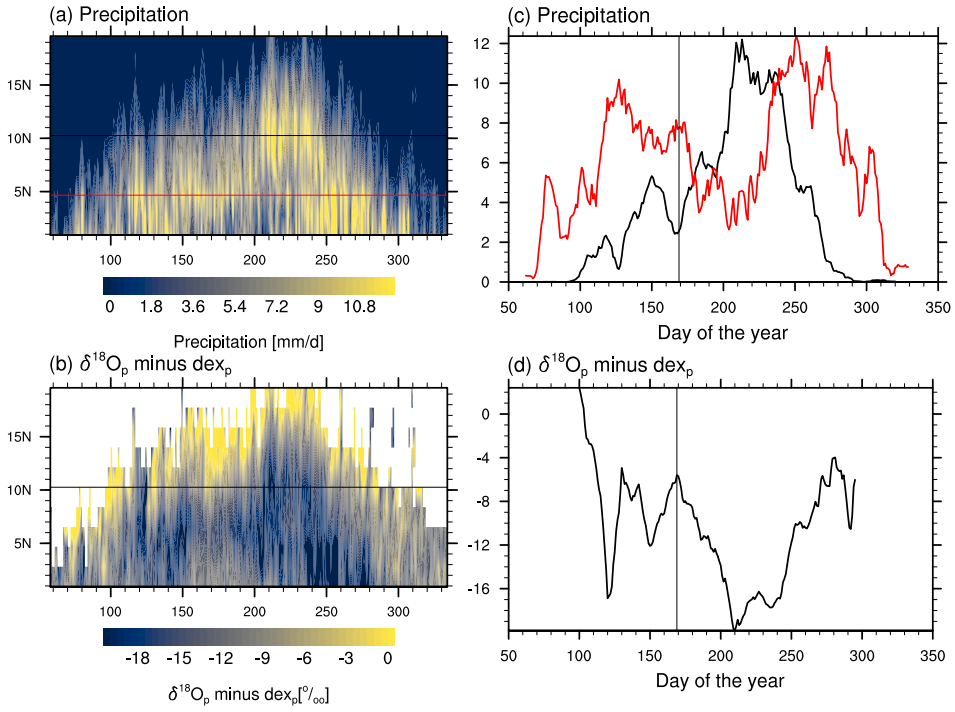


**Figure S5.** Simulated temporal time–latitude diagram of daily (a) precipitation and (b) $I$ averaged over 15°W - 20°E under MH climate condition for a specific year, with x-axis representing the day of the year and y-axis the latitude. (c) Time sections of precipitation averaged over 15°W - 20°E at 10.3°N (black line) and at 4.7°N (red line), filtered with high frequency variability (period less than 10 days) removed. (d) Time sections of $I$ averaged over 15°W - 20°E at 10.3°N, filtered with high frequency variability (period less than 10 days) removed.

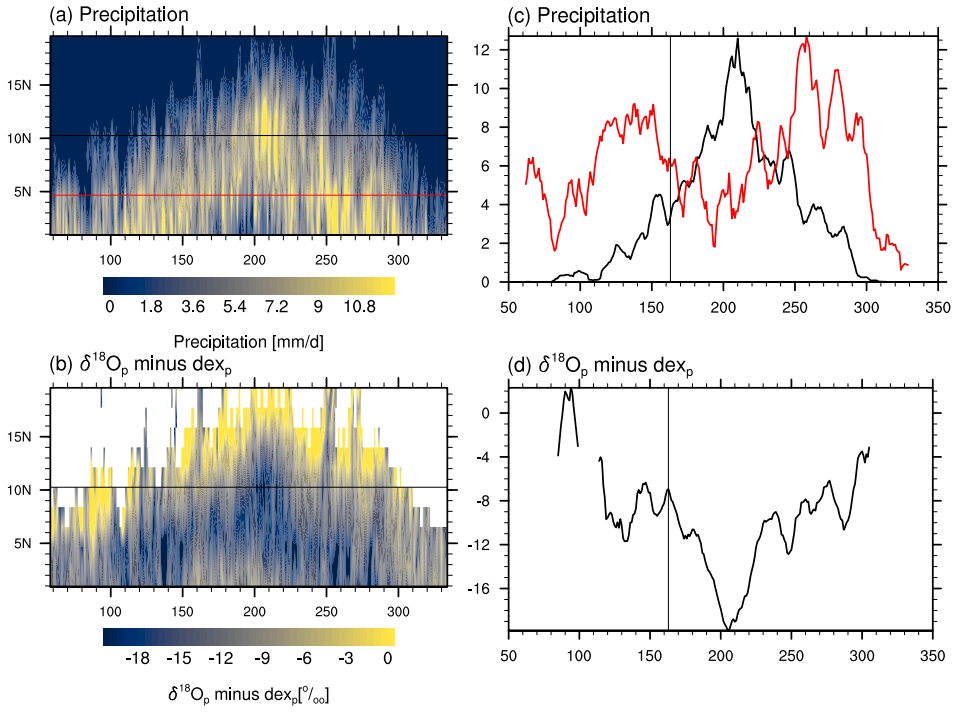


**Figure S6.** Simulated temporal time–latitude diagram of daily (a) precipitation and (b) $I$ averaged over 15°W - 20°E under MH climate condition for a specific year, with x-axis representing the day of the year and y-axis the latitude. (c) Time sections of precipitation averaged over 15°W - 20°E at 10.3°N (black line) and at 4.7°N (red line), filtered with high frequency variability (period less than 10 days) removed. (d) Time sections of $I$ averaged over 15°W - 20°E at 10.3°N, filtered with high frequency variability (period less than 10 days) removed.